The Use of a Long-Lifetime Component of Tryptophan to Detect Slow Orientational Fluctuations of Proteins

Klaus Döring,* Werner Beck,# Lars Konermann,* and Fritz Jähnig*
*Max-Planck-Institut für Biologie, Abteilung Membranbiochemie, D-72076 Tübingen, and #Universität Tübingen, Institut für Organische Chemie, D-72076 Tübingen, Germany

ABSTRACT The membrane protein porin and a synthetic polypeptide of 21 hydrophobic residues were inserted into detergent micelles or lipid membranes, and the fluorescence of their single tryptophan residue was measured in the time-resolved and polarized mode. In all cases, the tryptophan fluorescence exhibits a long-lifetime component of about 20 ns. This long-lifetime component was exploited to detect slow orientational motions in the range of tens of nanoseconds via the anisotropy decay. For this purpose, the analysis of the anisotropy has to be extended to account for different orientations of the dipoles of the short- and long-lifetime components. This is demonstrated for porin and the polypeptide solubilized in micelles, in which the longest relaxation time reflects the rotational diffusion of the micelle. When the polypeptide is inserted into lipid membranes, it forms a membrane-spanning α-helix, and the slowest relaxation process is interpreted as reflecting orientational fluctuations of the helix.

INTRODUCTION

The tryptophan fluorescence of proteins has a mean lifetime of a few nanoseconds (for a review see Beecham and Brand, 1985). Recently we have shown that for some proteins the fluorescence exhibits a long-lifetime component of about 25 ns (Döring et al., 1995). The proteins include membrane proteins and soluble proteins; in the latter case the tryptophan residue must be buried deeply in the protein. This lifetime component has a small amplitude, below 1%, but at long enough times it becomes dominant. Typically, at 40 ns the long-lifetime component becomes as strong as the short-lifetime components, and at longer times dominates them. A long-lifetime component is very useful for studying protein dynamics, especially slow motions in the range of tenths of nanoseconds. This requires measurement of the fluorescence intensity in the time-resolved and polarized mode, yielding the fluorescence anisotropy decay. Such measurements have been performed previously using extrinsic labels with long lifetimes (Dornmair and Jähnig, 1989). Such labels, however, always bear the danger of not accurately reflecting the dynamics of the unlabeled protein, and measurements using the intrinsic tryptophan fluorescence are therefore preferable. In the ideal case, single tryptophan proteins, either the wild type or a genetically engineered mutant, should be investigated.

The use of the long-lifetime component of tryptophan to detect slow fluctuations requires a modification of the standard analysis of the anisotropy decay. The reason for that lies in spectroscopic differences between the short- and long-lifetime components of the tryptophan fluorescence. This will be demonstrated for two systems, the membrane protein porin of *Rhodobacter capsulatus* and a synthetic hydrophobic 21-residue polypeptide (P21) that is an analog of alamethicin and contains a number of α-isobutyric acid residues (Voges et al., 1987). The native structure of porin is a trimer of β-barrels (Weiss et al., 1990), whereas polypeptide P21 in membranes forms a membrane-spanning α-helix (Voges et al., 1987). Both systems contain a single tryptophan residue. The modification of the analysis of the anisotropy decay will be worked out for porin and P21 solubilized in detergent micelles, in which the anisotropy is known to decay to zero at long times.

In the second part of the paper, the modified analysis of the anisotropy decay is employed to investigate the orientational fluctuations of a tryptophan fluorophore when it belongs to a membrane-spanning α-helix. Polypeptide P21 will be inserted into lipid membranes and the anisotropy decay will be analyzed.

Fluctuations of a helix have already been studied using the polypeptide melittin, which also bears a single tryptophan residue (John and Jähnig, 1988, 1992). However, melittin is associated with lipid membranes predominantly in the form of helices lying flat on the membranes (Frey and Tamm, 1991), and therefore its motion cannot be considered as representative of the motion of membrane-spanning helices that are often met in membrane proteins.

The polypeptide used by us has been characterized previously by time-resolved fluorescence anisotropy measurements (Vogel et al., 1988). However, the time window of 10 ns employed in these studies was too small to permit the detection of slow motions with high precision. This will be improved in the present paper by exploiting the long-lifetime component of the tryptophan fluorescence.

Received for publication 8 July 1996 and in final form 3 October 1996.

Address reprint requests to Dr. Klaus Döring, Max-Planck-Institut für Biologie, Abteilung Membranbiochemie, Corrensstrasse 38, D-72076 Tübingen, Germany. Tel.: 49-7071-601274; Fax: 49-7071-62971; E-mail: doering@mpib-tuebingen.mpg.de.

Dr. Konermann's present address is University of British Columbia, Department of Chemistry, Vancouver, BC V6T 1Z1 Canada.

0006-3495/97/01/326/09 $2.00

MATERIALS AND METHODS

Materials

The membrane protein porin was a gift of W. Welte (Universität Freiburg, Freiburg, Germany) and has been isolated and purified as described (Nestel et al., 1989). It occurs in the outer membrane of the bacterium *Rhodobacter capsulatus*, where it forms a trimer of membrane-spanning β-barrels, each comprising 301 residues (Weiss et al., 1990). It has only a single Trp residue at position 19, located at the upper rim of the β-barrel.

The polypeptide of 21 residues, called P21, was synthesized as described previously (Voges et al., 1987). Its sequence is H-(Ala-Aib-Ala-Aib-Ala)$_3$-Trp-(Ala-Aib-Ala-Aib-Ala)-O-Me, with Aib denoting aminoisobutyric acid. The Trp residue is at position 16.

The lipids 1,2-dimyristoylphosphatidylcholine (DMPC), 1,2-dimyristoylphosphatidylglycerol (DMPG), 1-palmitoyl-2-oleoylphosphatidylethanolamine (POPE), and 1-palmitoyl-2-oleoylphosphatidylglycerol (POPG) were obtained from Avanti Polar Lipids (Alabaster, AL). The detergent 1-*O*-*n*-dodecyl-β-D-maltoside (DM) was from Boehringer (Mannheim, Germany), and *n*-octyltetraoxyethylene (C_8E_4) was from Bachem (Heidelberg, Germany).

All solvents were of spectroscopic grade and were purchased from Merck (Darmstadt, Germany). Phenanthrene was obtained from Serva (Heidelberg, Germany), and *para*-terphenyl (PTP) was from Sigma (Munich, Germany). Lactose was purchased from Fluka (Buchs, Switzerland).

Sample preparation

The sample of porin was diluted into a 0.6% (w/v) solution of C_8E_4 buffered by 20 mM potassium phosphate at pH 8.0 with additional 200 mM NaCl and 1 mM $MgCl_2$. The final porin concentration was 10 μM.

The polypeptide samples were prepared from stock solutions of P21 in methanol (100 μM). The sample of P21 in butanol was prepared by diluting the stock solution of P21 in water-saturated butanol to a final concentration of 30 μM. The samples of P21 in DM micelles were prepared by diluting detergent stock solutions in methanol to a final concentration of 1.0 mM and adding P21 to reach a detergent/polypeptide mole ratio of 200/1. The samples with lipids were prepared from stock solutions of lipid in chloroform to reach a mole ratio of 100/1. Three different samples were prepared: 1) pure DMPC, 2) a mixture of DMPC and DMPG at a mole ratio of 80/20 (the negative charges of DMPG avoid vesicle fusion during the measurement), and 3) a mixture of POPE and POPG, again at a mole ratio of 80/20 (serving as a model system for the inner membrane of *Escherichia coli*). In all cases, the final lipid concentration was 3 mM. The solutions were tip-sonicated until a homogeneous distribution of vesicles with a mean radius of about 100 nm was reached. The vesicle size was controlled by quasi-elastic light scattering. The solutions were buffered at pH 7.4 by 10 mM potassium phosphate, in the presence of 100 mM NaCl.

The fluorescence standard PTP and the anisotropy standard phenanthrene were dissolved in cyclohexane. Their concentrations were 5 μM and 1 μM, respectively.

For each sample a control sample was prepared in the same way, except that the fluorescent substance was omitted.

The measurements were performed at room temperature unless stated otherwise.

Fluorescence measurements

The apparatus used has been described previously (Best et al., 1987; Döring et al., 1995). As the light source a mode-locked YAG laser and a cavity-dumped dye laser (Spectra Physics) with rhodamine 6G as dye were used. The final pulse repetition rate was 4.1 MHz. The wavelength of the excitation light was 300 nm, and its intensity could be varied by means of two polarizers, the first of which is rotatable and the second is fixed such that the polarization of the excitation light is perpendicular to the scattering plane. The fluorescence light was observed at right angles to the excitation light. It passed through a prism polarizer to select polarizations parallel and perpendicular to the initial polarization providing the intensities $i_{\parallel}(t)$ and $i_{\perp}(t)$. Thereafter, it passed through a long-pass filter (Schott, model WG345/4) and a monochromator (Kratos, model 1500) set at 350 nm and was detected by a photomultiplier tube (Philips, model XP2020Q) followed by single-photon counting electronics (EG&G). To avoid pulse pile-up, the count rate was kept below 1% of the pulse repetition rate (O'Connor and Phillips, 1984) and routinely was at 4×10^4 counts/s. In the multichannel analyzer, data were collected until typically 10^7 counts in the channel of maximum intensity were reached. The time window was usually set at about 65 ns by choosing a time-to-channel ratio of 131.6 ps/channel for 512 channels. A typical measurement took about 12 h, requiring high stability of the laser system.

The background samples to the samples were measured and corrected in the same way and their intensities $i_{\parallel,b}(t)$ and $i_{\perp,b}(t)$ subtracted from those of the samples $i_{\parallel,s}(t)$ and $i_{\perp,s}(t)$, yielding the polarized fluorescence intensities as $i_{\parallel}(t) = i_{\parallel,s}(t) - i_{\parallel,b}(t)$ and $i_{\perp}(t) = i_{\perp,s}(t) - i_{\perp,b}(t)$. The time courses of these intensities reflect three effects: 1) The time course of the exciting laser light, 2) the decays of the polarized fluorescence lights, and 3) the characteristics of the detection system. To extract the decays of the polarized fluorescence intensities 2) from the data, the effects of 1) and 3) have to be eliminated by deconvolution of $i_{\parallel}(t)$ and $i_{\perp}(t)$ with the apparatus response function. Because the experimental determination of the response function poses problems, it was avoided by employing a fluorescence standard with a strictly monoexponential decay (Wahl et al., 1974; Libertini and Small, 1984). We used PTP in cyclohexane with a lifetime of τ_S = 0.99 ns (Wijnaendts van Resandt et al., 1982).

The time courses of the deconvoluted polarized fluorescence intensities again represent a superposition of two effects: 1) the decay of the total fluorescence intensity and 2) the orientational motion of the fluorophore. The two effects are separated in a first approximation by determining the total fluorescence intensity $s(t) = i_{\parallel}(t) + 2Gi_{\perp}(t)$, with G denoting a correction factor for the polarization dependence of the monochromator, and the anisotropy $r(t) = (i_{\parallel}(t) - Gi_{\perp}(t))/(i_{\parallel}(t) + 2Gi_{\perp}(t))$. The correction factor G = 0.99 was determined by performing measurements on the fluorophore phenanthrene with a lifetime of about 15 ns in cyclohexane and requiring that its anisotropy at long times vanishes.

Data analysis

In cases in which the long-lifetime component plays no role, the data were analyzed by assuming for the total fluorescence intensity a multiexponential decay,

$$S(t) = \sum_{i=1}^{N} a_i \exp(-t/\tau_i), \tag{1}$$

and for the anisotropy a multiexponential decay plus a residual anisotropy at long times,

$$R(t) = \sum_{j=1}^{M} b_j \exp(-t/\phi_j) + R_\infty. \tag{2}$$

The components of the polarized fluorescence then follow as $I_{\parallel}(t) = S(t)[1 + 2R(t)]/3$ and $I_{\perp}(t) = S(t)[1 - R(t)]/3$. These quantities were convoluted with the apparatus response function (more exactly, its replacement by the fluorescence standard), and a nonlinear least-square fit to the experimental data for $i_{\parallel}(t)$ and $i_{\perp}(t)$ was performed by varying a_i, τ_i, b_i, ϕ_i, and R_∞. Visual rating of the residuals and a χ^2 test were taken as criteria for the best fit. We always started with monoexponential curves for the total fluorescence and the anisotropy and then included more exponentials stepwise until no further components were resolved, i.e., one lifetime or one relaxation time appeared twice. The partial amplitudes and the mean lifetime were obtained as $\alpha_i = a_i/\Sigma_j a_j$ and $\langle\tau\rangle = \Sigma_i \alpha_i \tau_i$, and the initial anisotropy as $R_0 = \Sigma_i b_i + R_\infty$.

The assumption of a multiexponential decay of the anisotropy as in Eq. 2 is justified, if the N different fluorescence transitions specified by their lifetimes τ_i share the same absorption and emission dipoles, so that effectively only one absorption and one emission dipole enter. In this case, explicit expressions for the initial and final anisotropies R_0 and R_∞ have been derived (Szabo, 1980; Zannoni, 1981):

$$R_0 = \frac{2}{5} P_2(\cos(\Theta_a - \Theta_e)) \quad (3)$$

$$R_\infty = \frac{2}{5} P_2(\cos \Theta_a) P_2(\cos \Theta_e) \langle P_2 \rangle^2. \quad (4)$$

Here, Θ_a and Θ_e are the angles of the absorption and emission dipoles relative to the symmetry axis of the fluorophore, $P_2(x) = (3x^2 - 1)/2$ denotes the second-order Legendre polynomial, and $\langle P_2 \rangle$ the orientational order parameter of the fluorophore defined as the average of $P_2(\cos[va])$ over the angular distribution of the fluorophore axis relative to its mean orientation (Jähnig, 1979). If the fluorescence transitions have different absorption and emission dipoles, the above relations require some modification. For simplicity, we consider the case of only two transitions and one relaxation process. The mixed anisotropy is then given by a generalization of the expression used by Valeur and Weber (1977):

$$R(t) = \frac{S_1(t)R_1(t) + S_2(t)R_2(t)}{S_1(t) + S_2(t)} \quad (5)$$

with

$$S_i(t) = a_i \exp(-t/\tau_i) \quad (6)$$

$$R_i(t) = b_i \exp(-t/\phi) + R_{\infty,i} \quad (7)$$

$$R_{0,i} = \frac{2}{5} P_2(\cos(\Theta_{a,i} - \Theta_{e,i})) \quad (8)$$

$$R_{\infty,i} = \frac{2}{5} P_2(\cos \Theta_{a,i}) P_2(\cos \Theta_{e,i}) \langle P_2 \rangle^2. \quad (9)$$

The expressions for the initial and final anisotropies become

$$R_0 = \alpha_1 R_{0,1} + \alpha_2 R_{0,2} \quad (10)$$

$$R_\infty = R_{\infty,2} \quad (\text{for } \tau_1 < \tau_2). \quad (11)$$

In the special case of an immobilized fluorophore, $\phi \gg \tau_i$, the time dependence of the anisotropy solely reflects the transition from one spectroscopic transition to the other:

$$R(t) = \frac{S_1(t)R_{0,1} + S_2(t)R_{0,2}}{S_1(t) + S_2(t)}. \quad (12)$$

The tryptophan fluorescence actually involves two excited states with different excitation and emission dipoles, state ^1L_a with excitation and emission dipoles parallel to each other and state ^1L_b with again excitation and emission dipoles parallel to each other, but roughly perpendicular to those of ^1L_a. Energetically, ^1L_b lies above ^1L_a and, therefore, is excited predominantly at 280 nm, whereas ^1L_a is excited predominantly at 300 nm. Measurements of the anisotropy with a time resolution of picoseconds indicate that at 300 nm ^1L_b is excited to a small extent followed by interconversion to ^1L_a within a few picoseconds (Ruggiero et al., 1990). This has two consequences: 1) detection of only one fluorescence lifetime and 2) partial depolarization of the fluorescence light, because the emission dipole of ^1L_a is roughly perpendicular to that of ^1L_b. Hence, within a few picoseconds the anisotropy decreases from 0.4 to a smaller value, e.g., 0.3 for an emission wavelength of 330 nm. From this value the contributions of the two transitions can be deduced. Insertion of $R_0 = 0.3$, $\Theta_{a,1} - \Theta_{e,1} = 0°$, and $\Theta_{a,2} - \Theta_{e,2} = \Theta_{a,2} - \Theta_{e,1} = 90°$ into Eqs. 8 and 10 leads to $\alpha_1 = 0.83$ and $\alpha_2 = 0.17$, in agreement with a previous estimate (Ichiye and Karplus, 1983).

In measurements without picosecond time resolution, an initial anisotropy of 0.3 is detected. This can be formally described in terms of one transition with a finite angle between excitation and emission dipoles. For $R_0 = 0.3$, Eq. 3 yields $\Theta_a - \Theta_e = 24°$ for this angle. This description will be used throughout the present paper.

Actually, the tryptophan fluorescence of proteins, even single-tryptophan proteins, contains more than one lifetime component. Typically, lifetimes of 0.5, 3, 6, and 10 ns are found (Gallay et al., 1993; Godik et al., 1993). They are postulated to arise from rotational isomers of the tryptophan side chains (Petrich et al., 1983; Wagner et al., 1987). This would imply that all of these lifetime components result from the same excited state (or spectroscopic combination of the two excited states ^1L_a and ^1L_b as discussed above). Therefore we assume that they share the same excitation and emission dipoles.

In previous measurements we demonstrated the existence of an additional long-lifetime component of about 25 ns in the tryptophan fluorescence of some proteins (Döring et al., 1995). In the present paper we will show that this component cannot be described by the same absorption and emission dipoles as the fast-lifetime components, because it exhibits an initial anisotropy (without a resolution of picoseconds) of about 0.05. Again, we do not know if this effect is a consequence of interconversion from ^1L_b to ^1L_a. If this were the case, the contribution of ^1L_b would be stronger than above. From Eq. 10, one would obtain $\alpha_1 = 0.42$ and $\alpha_2 = 0.58$. In any case, the anisotropy of the slow component will be described like that of the fast components, as arising formally from one transition. For $R_0 = 0.05$, the angle between excitation and emission dipoles is $\Theta_a - \Theta_e = 50°$.

In case the long-lifetime component plays a role, the data will be analyzed using Eq. 5, with the fast-lifetime components subsumed under one transition (denoted f for fast) and the slow component representing the other transition (denoted s for slow).

Theory of rotational diffusion

The measured relaxation times of the anisotropy may be interpreted within the framework of rotational diffusion of spheres or ellipsoids in isotropic or nonisotropic environments. The simplest case is given by rotational diffusion of a sphere in an isotropic viscous medium for which the anisotropy is given by (Memming, 1961; Tao, 1969; Belford et al., 1972)

$$R(t) = \frac{2}{5} P_2(\cos(\Theta_a - \Theta_e)) \exp(-6Dt), \quad (13)$$

with D denoting the coefficient of rotational diffusion,

$$D = k_B T/(6\eta V), \quad (14)$$

where V denotes the volume of the sphere and η the viscosity of the medium.

In the case of a symmetrical prolate ellipsoid in an isotropic viscous medium, the anisotropy becomes (Memming, 1961; Tao, 1969; Belford et al., 1972).

$$R(t) = \frac{2}{5}[g_0 \exp(-6D_\perp t) + g_1 \exp(-(5D_\perp + D_\parallel)t) + g_2 \exp(-(2D_\perp + 4D_\parallel)t)] \quad (15)$$

with the amplitudes

$$g_0 = \frac{1}{4}(3\cos^2\Theta_a - 1)(3\cos^2\Theta_e - 1) \quad (16)$$

$$g_1 = 3 \sin \Theta_a \cos \Theta_a \sin \Theta_e \cos \Theta_e \cos \Phi_{ae} \quad (17)$$

$$g_2 = \frac{1}{4}\sin^2\Theta_a \sin^2\Theta_e \cos(2\Phi_{ae}), \quad (18)$$

and the coefficients $D_\parallel$ and $D_\perp$ for rotational diffusion parallel and perpendicular to the axis of the ellipsoid

$$D_\parallel = \frac{3k_BT}{16\pi\eta a^3}\left(\left(\frac{a}{b}\right)^2 - \ln\left(\frac{2a}{b}\right)\right) \quad (19)$$

$$D_\perp = \frac{3k_BT}{16\pi\eta a^3}\left(2\ln\left(\frac{2a}{b}\right) - 1\right), \quad (20)$$

with a and b denoting the half-axes of the ellipsoid and $a \gg b$.

In the case of rotational diffusion or wobbling of a symmetrical ellipsoid in an ordering potential, an expression for the anisotropy has also been presented (van der Meer et al., 1984). It contains nine exponentials and a residual value. The amplitudes and relaxation times are functions of the six independent variables Θ_a, Θ_e, $\langle P_2\rangle$, $\langle P_4\rangle$, $D_\parallel$, and $D_\perp$. Here P_4 denotes the fourth-order Legendre polynomial $P_4(x) = (35x^4 - 30x^2 + 3)/8$ and $\langle P_4\rangle$ the fourth-order orientational order parameter, in analogy to the second-order orientational order parameter $\langle P_2\rangle$ introduced above. This theory has been applied to a fluorophore in lipid bilayers and has proved to be very successful (Best et al., 1987).

In adopting the theory of van der Meer et al. (1984) to tryptophan residues in proteins, one may assume that the fluctuations of the fluorophore are weaker than in the case of lipids, and the condition $\langle\vartheta^2\rangle \ll 1$ is fulfilled. Then the amplitudes and relaxation times may be expanded in powers of $\langle\vartheta^2\rangle$, e.g., $\langle P_2\rangle = 1 - (3/2)\langle\vartheta^2\rangle$. In lowest order of $\langle\vartheta^2\rangle$, a straightforward but tedious calculation leads to

$$R(t) = \frac{2}{5}\Big[\Big(3g_0 + \frac{5}{2}g_1 + g_2\Big)\langle\vartheta^2\rangle\exp(-t/\phi) + g_1\Big(1-\frac{5}{2}\langle\vartheta^2\rangle\Big)\exp(-D_\parallel t) + g_2(1-\langle\vartheta^2\rangle)\exp(-4D_\parallel t) + g_0(1-3\langle\vartheta^2\rangle)\Big], \quad (21)$$

with

$$\phi = \langle\vartheta^2\rangle/(2D_\perp). \quad (22)$$

It is easy to show that the initial and final anisotropies R_0 and R_∞ are still given by Eqs. 3 and 4.

Furthermore, one may introduce the assumption $D_\parallel = 0$, because the tryptophan residues can rotate about the membrane normal only together with the entire proteins, and this process is too slow to be detected in our measurements. This assumption alters the expression for the residual anisotropy to

$$R_\infty = \frac{2}{5}\Big[(g_0 + g_1 + g_2) - \Big(3g_0 + \frac{5}{2}g_1 + g_2\Big)\langle\vartheta^2\rangle\Big]. \quad (23)$$

To simplify the expression for $R(t)$ further, we take into account that for not too large Θ_a and Θ_e the condition $g_0 \gg g_1 \gg g_2$ is fulfilled and the term $(3g_0 + (5/2)g_1 + g_2)$ in Eqs. 21 and 23 may be replaced by $3(g_0 + g_1 + g_2) = 3P_2(\cos(\Theta_a - \Theta_e))$. For the ^1L_a transition with $\Theta_a = \Theta_e \approx 30°$ and $\Phi_{ae} = 0°$ (Ichiye and Karplus, 1983), the error made in this replacement is about 10%; for the ^1L_b transition with $\Theta_a \approx 60°$, $\Theta_e \approx 30°$, and $\Phi_{ae} = 180°$, it is even smaller. The expression for the anisotropy then simplifies to

$$R(t) = P_2(\cos(\Theta_a - \Theta_e))[\beta\exp(-t/\phi) + \beta_\infty], \quad (24)$$

with

$$\beta = \frac{2}{5}3\langle\vartheta^2\rangle \quad (25)$$

$$\beta_\infty = \frac{2}{5}(1 - 3\langle\vartheta^2\rangle) = \frac{2}{5}\langle P_2\rangle^2. \quad (26)$$

The initial anisotropy R_0 is still given by Eq. 3, whereas the final anisotropy R_∞ is no longer given by Eq. 4, but is proportional to the initial anisotropy, $R_\infty = R_0\langle P_2\rangle^2$. This contributes to the reduction of the number of independent variables in $R(t)$ from 6 to 3, $\Theta_a - \Theta_e$, $\langle\vartheta^2\rangle$ or $\langle P_2\rangle^2$, and $D_\perp$.

The above expression for $R(t)$ may easily be generalized to more than one relaxation process:

$$R(t) = P_2(\cos(\Theta_a - \Theta_e))\left[\sum_{j=1}^{M}\beta_j\exp(-t/\phi_j) + \beta_\infty\right], \quad (27)$$

with

$$\beta_j = \frac{2}{5}3\langle\vartheta_j^2\rangle \quad (28)$$

$$\beta_\infty = \frac{2}{5}\left(1 - \sum_{j=1}^{M}3\langle\vartheta_j^2\rangle\right) = \frac{2}{5}\prod_{j=1}^{M}\langle P_{2,j}\rangle^2 = \frac{2}{5}\langle P_{2,\mathrm{tot}}\rangle^2. \quad (29)$$

In the cases of rotational diffusion of a sphere and of wobbling motions of a symmetrical ellipsoid (Eqs. 13 and 27), the anisotropy exhibits a simple dependence on the absorption and emission dipoles: it is proportional to $P_2(\cos(\Theta_a - \Theta_e))$. Hence for these cases or a combination of them, the mixed anisotropy, Eq. 5, may be written as

$$R(t) = \frac{\alpha_f e^{(-t/\tau_f)}P_2(\cos(\Theta_{a,f} - \Theta_{e,f})) + \alpha_s e^{(-t/\tau_s)}P_2(\cos(\Theta_{a,s} - \Theta_{e,s}))}{\alpha_f e^{(-t/\tau_f)} + \alpha_s e^{(-t/\tau_s)}} * \left(\sum_{j=1}^{M}\beta_j e^{(-t/\phi_j)} + \beta_\infty\right). \quad (30)$$

Here the relaxational part is split off from the spectroscopic part. Such a simple description is not possible for the case of rotational diffusion of a symmetrical ellipsoid (Eq. 16).

RESULTS

Porin in detergent micelles

Fig. 1 shows the data obtained from a time-resolved and polarized measurement of the Trp fluorescence of porin in micelles of C_8E_4. The time courses of the intensity components $i_\parallel(t)$ and $i_\perp(t)$ are deduced as differences of the sample and background sample data, as shown in Fig. 1 *D*. It is obvious that the intensities decay rather homogeneously up to about 30 ns and thereafter decay more slowly. The anisotropy decays slowly at the beginning, but around 30 ns starts to decrease more rapidly until it levels off at a value around 0.05. The two intensities were fitted by assuming a multiexponential decay for the total intensity $S(t)$, Eq. 1, and

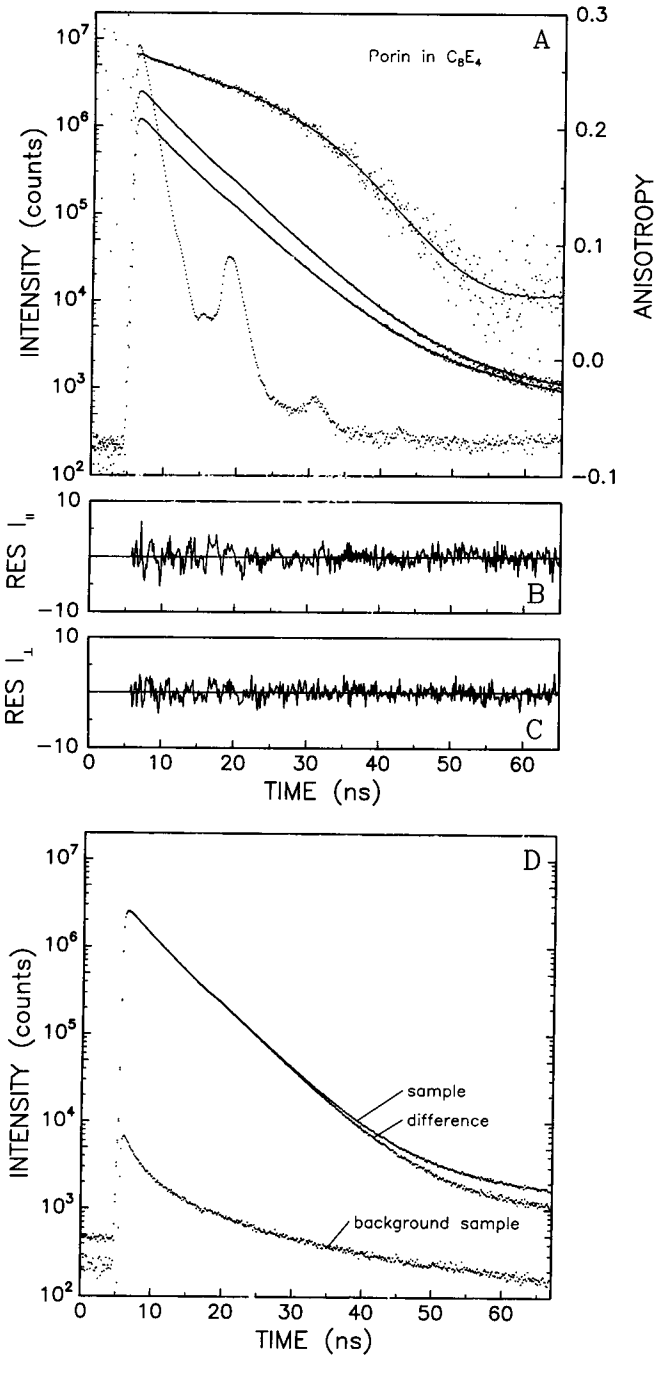

FIGURE 1 (*A*) Temporal decays of the fluorescence intensity components and of porin solubilized in micelles of the detergent C_8E_4 (*two curves in the middle*), of the corresponding fluorescence anisotropy $r(t)$ (*upper curve*), and of the exciting laser light (*lower curve*). The experimental data are shown (*dots*) together with the fits (*lines*) obtained by assuming a fourfold exponential decay for the total intensity $S(t)$ and a mixed anisotropy $R(t)$ according to Eq. 30, with one exponential and $R_\infty = 0$. (*B* and *C*) Residuals of $i_\parallel(t)$ and $i_\perp(t)$. (*D*) Measured intensities, $i_{\parallel,s}(t)$, $i_{\parallel,b}(t)$, and the difference $i_\parallel(t) = i_{\parallel,s}(t) - i_{\parallel,b}(t)$.

a mixed anisotropy $R(t)$ according to Eq. 30 with $R_\infty = 0$. The results obtained for $S(t)$ and $R(t)$ are listed in Table 1. The best results are obtained for $S(t)$, consisting of four exponentials, whereas $R(t)$ contains only one. Three lifetimes of the intensity lie in the range of a few nanoseconds and one around 20 ns. The amplitude of the slow component is only 0.4%. The single relaxation time of the anisotropy is 140 ns and probably corresponds to rotational diffusion of the porin/detergent micelles. This would imply that for porin solubilized in a micelle no internal motion of the Trp residue was detected.

The nonexponential time course of the anisotropy in Fig. 1 essentially reflects the transition from the fast-lifetime components to the long-lifetime component in the anisotropy as described by Eq. 12, because the relaxation time is large. The short- and long-lifetime components differ in the contribution of state ^1L_b to ^1L_a (see Materials and Methods) or, if the two components are described each in terms of one transition, in the effective angles between absorption and emission dipoles. For the fast component, the effective angle between the absorption and emission dipole results is $\Theta_{a,f} - \Theta_{e,f} = 27°$, and for the slow component it is $\Theta_{a,s} - \Theta_{e,s} = 51°$ (Table 1). It should be noted that the anisotropy of the background signal (data not shown) decays with a relaxation time of less than 1 ns. The leveling off at long times is caused by new excitations of the fluorescence due to incomplete suppression of the laser light after the pulse (Döring et al., 1995). Hence the decrease in the anisotropy due to rotational diffusion of the micelles is visible only at short times up to 20 ns.

To quantify the interpretation of the relaxation time of 140 ns as reflecting rotational diffusion of the mixed micelle, we assume the micelle to be spherical and to be composed of a porin trimer and detergent. According to the x-ray structure of porin (Weiss et al., 1990), the trimer may be considered a cylinder of radius 4 nm and height 5 nm, leading to a volume of $V_p = 250\ nm^3$ for the trimer. The number of detergent molecules associated with membrane proteins has been determined in a few cases (Møller and le Maire, 1993) and was found to be more compatible with a monolayer of detergent molecules covering the hydrophobic surface of the proteins than with a coverage in the form of a micelle. Adopting the monolayer model and the data available for the detergent $C_{12}E_8$, one estimates a number of 200 detergent molecules associated with a porin trimer occupying a volume of $V_d = 310\ nm^3$. Using Eqs. 13 and 14 with $V = V_p + V_d = 560\ nm^3$ and $\eta = 0.01$ p for water, one obtains $D = 1.2\ \mu s^{-1}$ and $\phi = 135$ ns. The nearly perfect agreement of the number for ϕ with the experimental result may be partially accidental, especially in view of the crude approximations under which it was derived, but nonetheless it strongly supports the notion that the observed relaxation process reflects rotational diffusion of a porin trimer surrounded by detergent molecules.

Polypeptide in butanol and detergent micelles

The results of time-resolved and polarized measurements on the polypeptide P21 in butanol are shown in Fig. 2. The time

TABLE 1 Results of fits of the temporal decay of the polarized components of the tryptophan fluorescence of porin in micelles of C_8E_4 and polypeptide P21 in various environments

		Porin in	Polypeptide P21 in					
		Micelles C_8E_4	Butanol	Micelles DM	Lipid DMPC T = 32°C	Lipid DMPC/PG T = 32°C	Lipid DMPC/PG T = 10°C	Lipid POPE/PG
τ_1	(ns)	0.5	0.2	0.3	0.2	0.4	0.5	0.5
τ_2		—	1.7	1.3	1.5	1.5	2.1	1.5
τ_3		2.3	4.4	3.2	4.0	3.6	5.2	3.1
τ_4		5.6	6.3	6.7	7.2	6.1	8.9	5.4
τ_5		19.2	23.6	21.4	30.8	22.4	—	26.7
α_1		0.06	0.01	0.30	0.16	0.05	0.13	0.33
α_2		—	0.20	0.18	0.29	0.26	0.32	0.33
α_3		0.14	0.33	0.25	0.44	0.47	0.39	0.25
α_4		0.80	0.45	0.27	0.10	0.22	0.16	0.09
α_5		0.004	0.002	0.004	0.002	0.002	—	0.001
$\langle\tau\rangle$	(ns)	4.7	4.7	3.0	3.0	3.5	4.2	2.0
ϕ_1	(ns)	—	0.4	0.6	0.4	0.3	—	0.1
ϕ_2		—	1.4	2.2	1.6	1.8	1.9	1.8
ϕ_3		140	2.9	20.5	12.0	12.5	18.6	10.6
β_1		—	0.080	0.058	0.009	0.022	—	0.107
β_2		—	0.237	0.068	0.076	0.078	0.042	0.071
β_3		0.4	0.082	0.274	0.205	0.195	0.103	0.102
β_∞		0	0	0	0.110	0.106	0.255	0.120
$\theta_{af} - \theta_{ef}$		27°	34°	31°	33°	32°	31°	33°
$\theta_{as} - \theta_{es}$		51°	—	—	50°	52°	—	51°
R_0		0.28	0.21	0.24	0.22	0.23	0.24	0.23
R_∞		0	0	0	0.015	0.008	0.15	0.012
χ^2		2.0	2.1	2.6	2.9	4.7	2.7	4.1

Fits were made assuming for the total intensity $S(t)$ a multiexponential decay (as in Eq. 1) and for the anisotropy $R(t)$ a mixed expression (as in Eq. 30), except for P21 in butanol and in DM, where a multiexponential decay (as in Eq. 2) was assumed.

course of the total intensity $s(t)$ indicates the existence of a long-lifetime component, whereas the anisotropy $r(t)$ decays to zero within less than 10 ns. This implies that in this case the long lifetime is not necessary to analyze the anisotropy. Therefore, the data were fitted by assuming multiexponential decays for $S(t)$ and $R(t)$ (Eqs. 1 and 2); the results are included in Table 1. The long lifetime is 23.6 ns with an amplitude of 0.2%. The anisotropy is fitted best by three exponentials with the relaxation times 0.4, 1.4, and 2.9 ns.

Attempting to assign these times to relaxation processes, we note that the peptide in a hydrophobic medium forms an α-helix (Vogel et al., 1988) and consider the α-helix as an ellipsoid with half-axes a = 1.57 nm and b = 0.63 nm, in analogy to the case of alamethicin (Schwarz and Savko, 1982). Then, Eqs. 19 and 20 with η = 0.025 p for butanol yield $D_\parallel$ = 118 μs^{-1} and $D_\perp$ = 57 μs^{-1}, which after insertion into Eq. 15 yield the relaxation times 1.7, 2.5, and 2.9 ns. These numbers lie in the range of the longest measured relaxation time of 2.9 ns, providing evidence for the assignment of this relaxation time to rotational diffusion of the polypeptide. The two measured relaxation times of 0.4 and 1.4 ns were also found in the case of P21 in a lipid bilayer (see below) and, therefore, are assigned to internal fluctuations of the tryptophan side chains relative to the helix backbone. But, whereas the amplitude of the second relaxation process in all other cases is approximately as low as 0.07, here the larger amplitude of 0.237 may be interpreted to represent an overlay of internal motion and rotational motion of the entire polypeptide. That only two of the three relaxation times predicted for an ellipsoid are observed may be caused by either the three relaxation times not being resolved in our measurements or the polypeptide being more spherical than assumed.

The results obtained for P21 in micelles of DM are shown in Fig. 3. The total intensity $s(t)$ again indicates the existence of a long-lifetime component, the anisotropy $r(t)$ decays more slowly than for P21 in butanol, and the long-lifetime component seems to have an influence. The increase in $r(t)$ at long times is again caused by new excitations of the fluorescence. The results of fits by multiexponentials for $S(t)$ and $R(t)$ (Eqs. 1 and 2) are included in Table 1. The long lifetime is 21.4 ns, with an amplitude of 0.4%. The best fit of the anisotropy is obtained with three exponentials, the longest relaxation time being 20.5 ns. The effective angle between the absorption and emission dipoles is obtained as $\Theta_{a,f} - \Theta_{e,f} = 31°$ for the fast lifetime component, whereas the angle for the slow component is not resolvable, similar to the case of P21 in butanol.

The long relaxation time may be interpreted in the same manner as the relaxation time of porin in detergent micelles. Adopting again the monolayer model and the data available for DM (Møller and le Maire, 1993), one obtains 110 molecules of DM associated with the helix, occupying a volume of V_d = 110 nm^3. The volume of the helix is

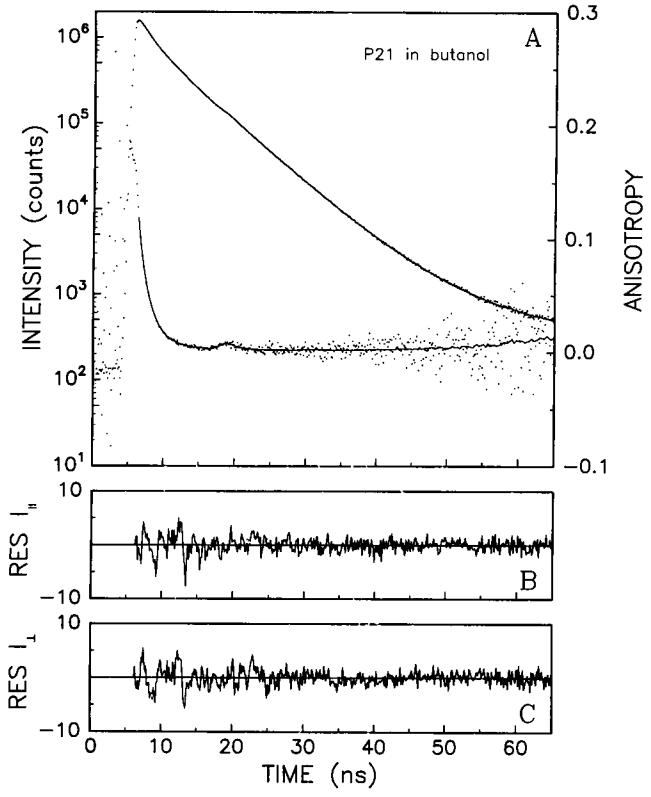

FIGURE 2 (*A*) Temporal decays of the total fluorescence intensity $s(t)$ of polypeptide P21 in butanol (*upper curve*) and of the fluorescence anisotropy $r(t)$ (*lower curve*). The experimental data are shown (*dots*), together with the fits (*lines*) obtained by assuming a fivefold exponential decay for the total intensity $S(t)$ and a threefold exponential decay for the anisotropy $R(t)$. (*B* and *C*) Residuals of $i_{\parallel}(t)$ and $i_{\perp}(t)$.

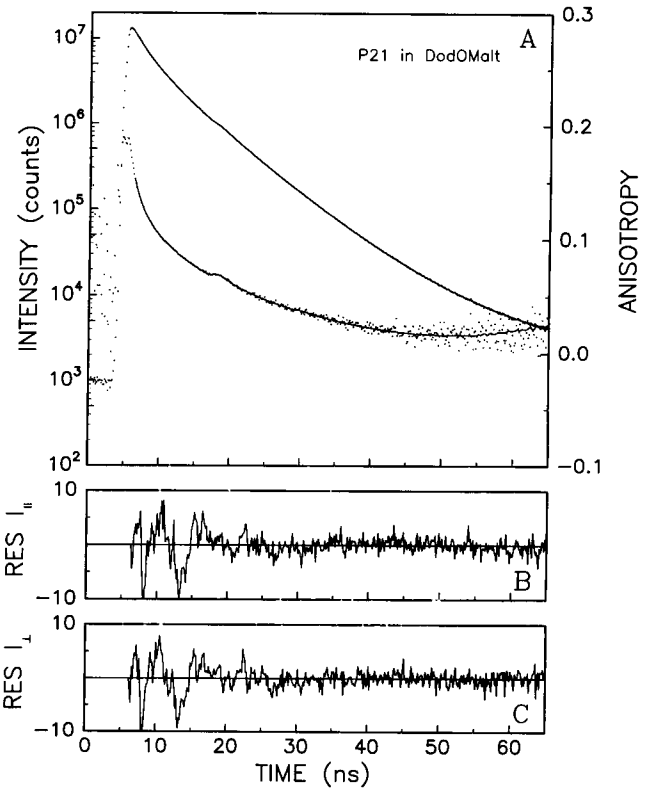

FIGURE 3 (*A*) Temporal decays of the total fluorescence intensity $s(t)$ of polypeptide P21 solubilized in micelles of the detergent DM (*upper curve*) and of the fluorescence anisotropy $r(t)$ (*lower curve*). The experimental data are shown (*dots*), together with the fits (*lines*) obtained by assuming a fivefold exponential decay for the total intensity $S(t)$ and a mixed anisotropy $R(t)$ according to Eq. 2, with one exponential and $R_\infty = 0$. (*B* and *C*) Residuals of $i_{\parallel}(t)$ and $i_{\perp}(t)$.

relatively small, $V_p = 2$ nm^3, and Eqs. 13 and 14 lead to $D = 6\ \mu s^{-1}$ and a relaxation time $\phi = 28$ ns. Roughly the same numbers are obtained when instead of the monolayer model one assumes the helix to be surrounded by detergent molecules in the form of a micelle. It may be noted that the aggregation number of pure DM in micelles is also 110. The good agreement of the estimate for ϕ with the experimental result lends support to the assignment of the slow relaxation process to rotational diffusion of helix/detergent micelles. The two short relaxation times of 0.6 and 2.2 ns again may be assigned to fluctuations of the tryptophan side chains relative to the helix backbone.

As a control, the measurements on P21 in DM micelles were repeated in the presence of varying amounts of lactose, thereby increasing the viscosity of the medium. The two short relaxation times remained essentially unaltered, but the long relaxation time increased, as shown in Fig. 4. The solution with the highest lactose concentration had a viscosity of $\eta = 1.6$ cp (*Handbook of Physics and Chemistry*, 54th ed), i.e., lactose increased η by a factor of 1.6, and ϕ_3 increased by the same factor. This linear increase in ϕ_3 with the viscosity η is in agreement with Eqs. 13 and 14 and thus lends further support to the interpretation of the slow relaxation process as rotational diffusion of helix/detergent micelles.

Polypeptide in lipid membranes

The results of measurements on P21 inserted into lipid membranes of DMPC at 32°C are shown in Fig. 5. The total intensity $s(t)$ exhibits a behavior similar to that in the case of P21 in DM micelles. The anisotropy $r(t)$ also decays in a similar way, but no longer approaches zero at long times. This indicates a residual orientational order of the fluorophore at long times. The results of fits by multiexponentials for $S(t)$ (Eq. 1) and a mixed anisotropy $R(t)$ (Eq. 30) are again included in Table 1. The long lifetime is 30.8 ns, higher than for DM micelles; the amplitude is again 0.2%. The anisotropy is best fitted by assuming three exponentials and a residual value at long times. The longest relaxation time is 12.0 ns and the residual anisotropy is 0.015.

In attempting to interpret the slow relaxation process, one may assume that it reflects rotational diffusion of the helix in an ordering potential. From the amplitude β_3, the orientational fluctuations for this slow process result as $\langle \vartheta^2 \rangle = 0.17$ or $\langle \vartheta^2 \rangle^{1/2} = 24°$, equivalent to an orientational order parameter $\langle P_2 \rangle = 0.75$. Insertion into Eq. 22 leads to $D_\perp = 7.1\ \mu s^{-1}$. This value is smaller than the value obtained for $D_\perp$ in butanol by a factor of about 8. This implies that the

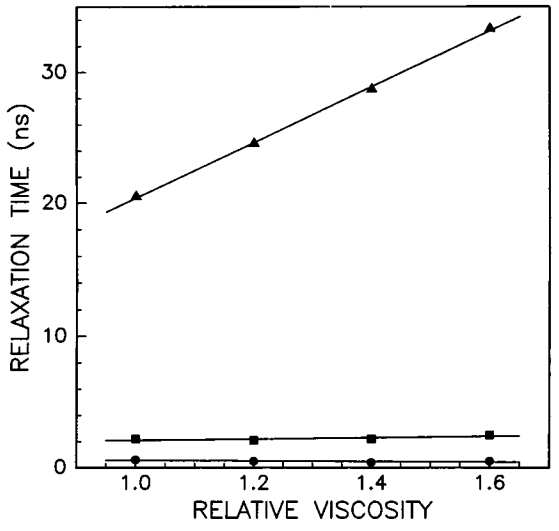

FIGURE 4 Variation of the relaxation times for P21 in DM micelles with the viscosity of the medium. The viscosity was varied by adding lactose to reach concentrations of 6.6%, 11.3%, and 14.9% (w/w). The measurements were performed at 20°C. Whereas the long relaxation time shows a linear increase with the viscosity, the two short times remain nearly constant.

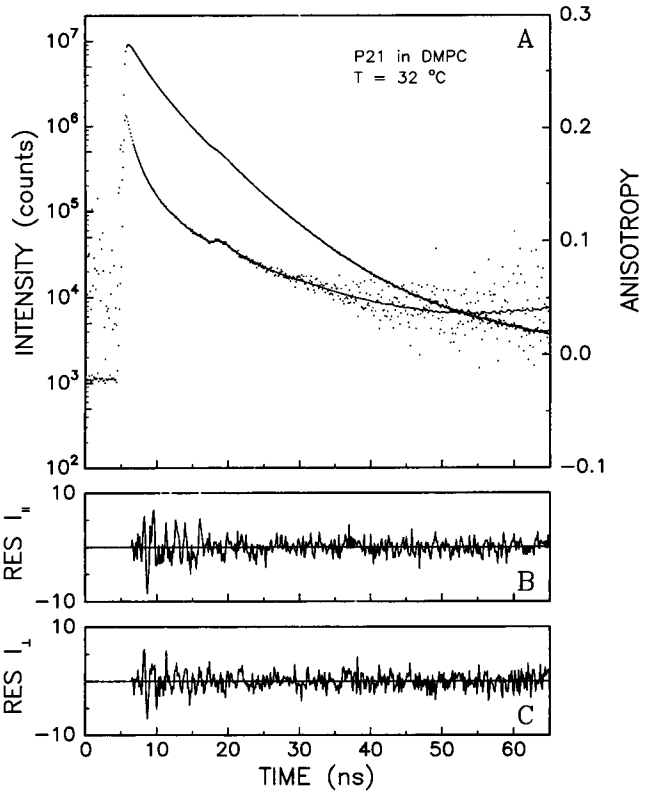

FIGURE 5 (*A*) Temporal decays of the total fluorescence intensity $s(t)$ of polypeptide P21 inserted in vesicle membranes of DMPC at 32°C (*upper curve*) and of the fluorescence anisotropy $r(t)$ (*lower curve*). The experimental data are shown (*dots*) together with the fits (*lines*) obtained by assuming a fivefold exponential decay for the total intensity $S(t)$ and a mixed anisotropy $R(t)$ according to Eq. 30, with one exponential and a finite R_∞. (*B* and *C*) Residuals of $i_{\parallel}(t)$ and $i_{\perp}(t)$.

viscosity in a lipid membrane is about 8 times higher than in butanol; hence $\eta = 0.2$ p in a fluid lipid membrane. A value of $\eta = 0.2$ p has been determined previously for the viscosity governing the orientational fluctuations of the fluorophore diphenylhexatriene in fluid lipid membranes (Best et al., 1987). The agreement between the two viscosities lends support to the notion that the slow process detected reflects orientational fluctuations of a membrane-spanning α-helix. By consequence, the two faster relaxation processes would then be assigned to internal fluctuations, wobbling motions, of the tryptophan side chains relative to the helix backbone.

Similar results were obtained with other lipids, as listed in Table 1. In one case, the negatively charged lipid DMPG was added to DMPC; in another case the mixture POPE/POPG was used, which represents a good model system for *E. coli* inner membrane lipids. A different behavior was found only when the temperature was below the lipid phase transition. Here the long-lifetime component was absent, but the mean lifetime was sufficiently long to permit measurement of the anisotropy over 65 ns. The analysis of the anisotropy leads to slow orientational fluctuations, with $\langle \vartheta^2 \rangle = 0.09$ corresponding to $\langle P_2 \rangle = 0.87$ and a diffusion coefficient $D_\perp = 2.4\ \mu s^{-1}$. This value of $D_\perp$ indicates that the viscosity in the ordered phase of lipids is higher than in the fluid phase by a factor of about 3.

DISCUSSION

When the long-lifetime component of about 20 ns of the tryptophan fluorescence of proteins is employed to detect slow motions, a new observation is made. The anisotropy decay is not uniform, even when only one kind of motion exists (Fig. 1). The reason for this behavior is spectroscopic in origin; the absorption and emission dipoles of the short- and long-lifetime components differ in their orientation so that the anisotropy changes when the long-lifetime component comes into play. If the fast and slow components are each described as originating from one transition, the angle between the absorption and emission dipoles is about 32° for the fast and about 51° for the slow transition.

From these studies one can draw two conclusions: 1) When the long-lifetime component of the tryptophan fluorescence is exploited, the experimental time window may be extended to several tens of nanoseconds and motions with typical times of the order of 100 ns may be detected. This holds for the case that no fast motions exist. If they do exist, the typical time of the detectable slow motions must lie below 100 ns. The price one has to pay for the detection of such slow motions is the long measuring time necessary to get a high enough signal/noise ratio at long times. 2) The typical time of the slow motions can be determined with an accuracy of about 20%, as exemplified by the change in the relaxation time for rotational diffusion of a polypeptide/detergent micelle when the viscosity of the medium is changed.

The long-lifetime component of the tryptophan fluorescence together with a modified analysis of the anisotropy was used to study the orientational motion of the tryptophan residue of P21 when the polypeptide is inserted into a lipid membrane and forms a membrane-spanning α-helix. Three relaxation processes were detected with typical times of 0.4, 1.6, and 12 ns for the lipid DMPC in the fluid phase. Similar results were obtained with other lipids in the fluid phase, whereas in the ordered lipid phase the long relaxation time increased. Vogel et al. (1988), in their study of the same polypeptide in the fluid phase of DMPC, found two relaxation times, 0.4 ns and 8.9 ns. They used a time window of 10 ns and did not profit from the long-lifetime component of the tryptophan fluorescence. Obviously they could not resolve the two relaxation times of 1.6 ns and 12 ns detected in our measurements, which demonstrates the improvement gained upon exploiting the long-lifetime component.

It is not possible at the present stage to assign the three relaxation processes observed with the polypeptide P21 in a lipid membrane to distinct orientational motions of the tryptophan fluorophore. An attempt was made to interpret the slowest relaxation process with 12 ns as orientational fluctuations of the membrane-spanning α-helix formed by P21. The two faster relaxation processes might then reflect orientational fluctuations of the tryptophan side chain relative to the α-helix. The fastest (with 0.4 ns) may correspond to wobbling fluctuations of the side chain due to small changes of the dihedral angles, and the other (with 1.6 ns) to larger fluctuations due to isomerizations of the side chain dihedral angles. However, further studies are required to put this interpretation on a firm basis. These studies may include molecular dynamics simulations, which have recently been extended into the nanosecond time range. The experimental data presented here may serve as useful controls for such simulations.

We thank E. John and T. Surrey from this institute, G. Jung from the University of Tübingen for stimulating discussions, and W. Welte from the University of Freiburg for the gift of porin.

REFERENCES

Beecham, J. M., and L. Brand. 1985. Time-resolved fluorescence of proteins. *Annu. Rev. Biochem.* 54:43–71.

Belford, G. G., R. L. Belford, and G. Weber. 1972. Dynamics of fluorescence polarization in macromolecules. *Proc. Natl. Acad. Sci. USA.* 69:1392–1393.

Best, L., E. John, and F. Jähnig. 1987. Order and fluidity of lipid membranes as determined by fluorescence anisotropy decay. *Eur. Biophys. J.* 15:87–102.

Dornmair, K., and F. Jähnig. 1989. Internal dynamics of lactose permease. *Proc. Natl. Acad. Sci. USA.* 86:9827–9831.

Döring, K., L. Konermann, T. Surrey, and F. Jähnig. 1995. A long lifetime component in the tryptophan fluorescence of some proteins. *Eur. Biophys. J.* 23:423–432.

Frey, S., and L. Tamm. 1991. Orientation of melittin in phospholipid bilayers. *Biophys. J.* 60:922–930.

Gallay, J., M. Vincent, I. M. L. de la Sierra, J. Alvarez, R. Ubieta, J. Madrazo, and G. Padron. 1993. Protein flexibility and aggregation state of human epidermal growth factor. *Eur. J. Biochem.* 211:213–219.

Godik, V. I., R. E. Blankenship, T. P. Causgrove, and N. Woodbury. 1993. Time-resolved tryptophan fluorescence in photosynthetic reaction centers from Rhodobacter sphaeroides. *FEBS Lett.* 321:229–232.

Ichiye, T., and M. Karplus. 1983. Fluorescence depolarisation of tryptophan residues in proteins: a molecular dynamics study. *Biochemistry.* 22:2884–2893.

Jähnig, F. 1979. Structural order of lipids and proteins in membranes: evaluation of fluorescence anisotropy data. *Proc. Natl. Acad. Sci. USA.* 76:6361–6365.

John, E., and F. Jähnig. 1988. Dynamics of melittin in water and membranes as determined by fluorescence anisotropy decay. *Biophys. J.* 54:817–827.

John, E., and F. Jähnig. 1992. A synthetic analogue of melittin aggregates in large oligomers. *Biophys. J.* 63:1536–1543.

Libertini, L. J., and E. W. Small. 1984. F/F deconvolution of fluorescence decay data. *Anal. Biochem.* 138:314–318.

Memming, R. 1961. Theorie der Fluoreszenzpolarisation für nicht kugelsymmetrische Moleküle. *Z. Phys. Chem.* 28:168–189.

Møller, J. V., and M. le Maire. 1993. Detergent binding as a measure of hydrophobic surface area of integral membrane proteins. *J. Biol. Chem.* 25:18659–18672.

Nestel, U., T. Wacker, D. Woitzek, J. Weckesser, W. Kreutz, and W. Welte. 1989. Crystallization and preliminary X-ray analysis of porin from *Rhodobacter capsulatus*. *FEBS Lett.* 242:405–408.

O'Connor, D. V., and D. Phillips. 1984. *In* Time-Correlated Single Photon Counting. Academic Press, London.

Petrich, J. W., M. C. Chang, D. B. McDonald, and G. R. Fleming. 1983. On the origin of nonexponential fluorescence decay in tryptophan and its derivatives. *J. Am. Chem. Soc.* 105:3824–3832.

Ruggiero, A. J., D. C. Todd, and G. R. Fleming. 1990. Subpicosecond fluorescence anisotropy studies of tryptophan in water. *J. Am. Chem. Soc.* 112:1003–1014.

Schwarz, G., and P. Savko. 1982. Structural and dipolar properties of the voltage-dependent pore former alamethicin in octanol/dioxane. *Biophys. J.* 39:211–219.

Szabo, A. 1980. Theory of polarized fluorescent emission in uniaxial liquid crystals. *J. Chem. Phys.* 72:4620–4626.

Tao, T. 1969. Time-dependent fluorescence depolarization and Brownian rotational diffusion coefficients of macromolecules. *Biopolymers.* 8:609–632.

Valeur, B., and G. Weber. 1977. Resolution the fluorescence excitation spectrum of indole into ^1L_a and ^1L_b excitation bands. *Photochem. Photobiol.* 25:441–444.

van der Meer, W., H. Pottel, W. Herreman, M. Ameloot, H. Hendricks, and H. Schröder. 1984. Effect of orientational order on the decay of the fluorescence anisotropy in membrane suspensions. *Biophys. J.* 46: 515–523.

Vogel, H., L. Nilsson, R. Rigler, K. P. Voges, and G. Jung. 1988. Structural fluctuations of a helical polypeptide traversing a lipid bilayer. *Proc. Natl. Acad. Sci. USA.* 85:5067–5071.

Voges, K. P., G. Jung, and W. H. Sawyer. 1987. Depth-dependent fluorescent quenching of a tryptophan residue located at defined positions on a rigid 21-peptide helix in liposomes. *Biochim. Biophys. Acta.* 896: 64–76.

Wagner, B. D., D. R. James, W. R. Ware. 1987. Fluorescence lifetime distribution in homotryptophan derivatives. FEBS Lett. 138:181–184.

Wahl, P., J. C. Auchet, and B. Donzel. 1974. The wavelength dependence of the response of a pulse fluorimeter using the single photoelectron counting method. *Rev. Sci. Instrum.* 45:28–32.

Weiss, M. S., T. Wacker, J. Weckesser, W. Welte, and G. Schulz. 1990. The three-dimensional structure of porin from *Rhodobacter capsulatus* at 3 Å resolution. *FEBS Lett.* 267:268–272.

Wijnaendts van Resandt, R. W., R. H. Vogel, and S. W. Provencher. 1982. Double beam fluorescence lifetime spectrometer with subnanosecond resolution: application to aqueous tryptophan. *Rev. Sci. Instrum.* 53: 1392–1397.

Zannoni, C. 1981. A theory of fluorescence depolarization in membranes. *Mol. Phys.* 42:1303–1320.